

Electrostatic Spinning and Properties of Ultrafine Fibers

G.C. Rutledge, Y. Li, S. Fridrikh
*Department of Chemical Engineering
Massachusetts Institute of Technology, Cambridge, MA 02139*

S.B. Warner, V.E. Kalayci, P. Patra
*Department of Textile Sciences, University of Massachusetts Dartmouth,
Dartmouth, MA 02747*

Abstract

Electrospinning is a process that offers unique capabilities for producing novel synthetic fibers of unusually small diameter and good mechanical performance (“nanofibers”), and fabrics with controllable pore structure and high surface area. While the process of electrospinning has been known for over half a century, current understanding of the process, and those parameters that influence the properties of the fibers produced, is very limited. In this work, we evaluate the effects of processing parameters: electric field, flow rate and electric current, and solution properties, such as conductivity, on the morphology of the fibers formed. In addition, porosity and pore size distribution have been measured.

Objectives

The objective of this project is the development of the fundamental engineering science and technology of electrostatic fiber production (“electrospinning”) and the performance of materials derived therefrom. Begun in May 2001 as the successor to Project M98-D01, this project aims to achieve the following goals:

- Extend our current understanding of electrohydrodynamics and the development of fluid instabilities in electrospinning to account for such important effects as mass and heat transport and polymer viscoelasticity.
- Control fiber diameter through choice of solution properties, operating parameters and equipment design.
- Evaluate methods for introducing electrostatic charge to solutions and for manipulating local electric fields along the spin line.
- Improve productivity of the electrospinning process.
- Develop methods for characterizing both fiber and fabric properties, especially mechanical properties, molecular orientation, porosity and specific surface area.

Introduction

Conventional fiber spinning techniques, e.g. melt spinning, dry spinning or wet spinning, rely on mechanical forces to produce fibers by extruding polymer melt or solution through a spinnerette and subsequently drawing the resulting filaments as they solidify or coagulate. Electrospinning offers a fundamentally different approach to fiber production by introducing electrostatic forces to modify the fiber formation process. Although the idea goes back at least 60 years [1], exploitation of technologies based on electrospinning have been very limited, due to poor understanding of the process and consequent limitation in process control, reproducibility and productivity. Interest has renewed in recent years with the work of Reneker and co-workers, who have demonstrated electrospinning for a wide variety of materials and solutions [2,3] and have

produced a number of different and interesting fiber structures and morphologies [3-5]. Notable among these are fiber of extremely small diameters (40 nm in the case of electrospun poly(p-phenylene terephthalamide), or Kevlar, fibers) [3] and “beaded” fibers [6,7]. Larrondo and Manley were the first to demonstrate electrospinning of polyethylene and polypropylene fibers from the melt [8,9]. Permeability studies on electrospun fabrics indicate potential for membrane and filtration applications [10]. Electrospun fabrics have also been shown to impart some improved mechanical performance characteristics in rubber and epoxy matrix composites [11].

The basic process of electrospinning involves the introduction of electrostatic charge to a stream of polymer melt or solution in the presence of a strong electric field. The predominant form of operation entails charge induction in the fluid through contact with a high voltage electrode in a simple metal or glass capillary spinnerette. Relaxation of the induced charge to the free surface of the fluid upon exiting the spinnerette results in the formation of a Taylor cone and ejection of a single jet of charged fluid. The charged jet accelerates and thins in the electric field, ultimately impacting and collecting on a grounded device, typically a plate or belt. Under certain conditions of operation, the fluid jet becomes unstable before it reaches the collector. With low molecular weight fluids, the onset of instability typically results in a spray of small, charged droplets, in a process known as “electrospraying”. With polymeric fluids, viscoelastic forces stabilize the jet, permitting the formation of small diameter, charged filaments that appear as an “envelope” or cone of dispersed fluid, and that solidify and deposit on the collector in the form of a nonwoven fabric. Under these conditions, it is common to observe mean fiber diameters on the order of 0.1 μm , three orders of magnitude smaller than the diameter of the jet entering the unstable region (100 μm), and well below the diameter of conventional extruded fibers (10-100 μm).

In our previous work, we have recently shown that the jet formation and thinning prior to the onset of instability can be predicted quantitatively from fluid properties (e.g. viscosity and conductivity), operating parameters (electric field and flow rate) and spinnerette geometry. We have further shown that the fluid instability is convective, and can be predicted from knowledge of how the jet diameter and surface charge vary along the length of the jet. The challenge remains to address the effect of the variables mentioned above on the sub-micron fiber structure and morphology. The purpose of the current work is to look systematically at the effects of process parameters, such as flow rate, electric field and solution conductivity, on the structure and morphology of electrospun fibers. Mathematical models are being developed to predict fiber morphology.

Experimental

1. Equipment Design

Electrospinning equipment has been fabricated at both sites collaborating on this proposal, University of Massachusetts at Dartmouth (UMD) and Massachusetts Institute of Technology (MIT). In addition to conventional test equipment consisting of simple fluid reservoirs connected to a high voltage power supply, specialized designs have also been constructed for the purposes of (a) studying simple electrohydrodynamic flows amenable to mathematical analysis (MIT) and (b) investigating methods for increasing the productivity of electrospinning (UMD).

The electrospinner design used for study of electrohydrodynamic flows at MIT has been described in detail previously [12]. The configuration in use at UMD is illustrated in Figure 1. Flow rate is controlled using a syringe pump. Applied voltage is regulated up to 30 kV using a dc power supply. Typical operating regimes are flow rates between 0.05 and 2 ml/min, voltages between 10 and 20 kV, and spinnerette-to-collector distance of 10 to 20 cm. The UMD configuration is modified with a Faraday cup and ammeter for measuring current and charge. The fibers are spun on to a non-conductive polyethylene film and transferred to the Faraday cup immediately after spinning, where the charge on the fiber is measured using a nanocoulomb meter. After charge measurement the substrate is weighed using a digital balance, and the resulting measurements used to determine the charge per unit mass. These results may then be compared to similar measurements made at MIT, where the charge per unit volume is determined from the electric current and flow rate measured during steady state operation of the electrospinner [13].

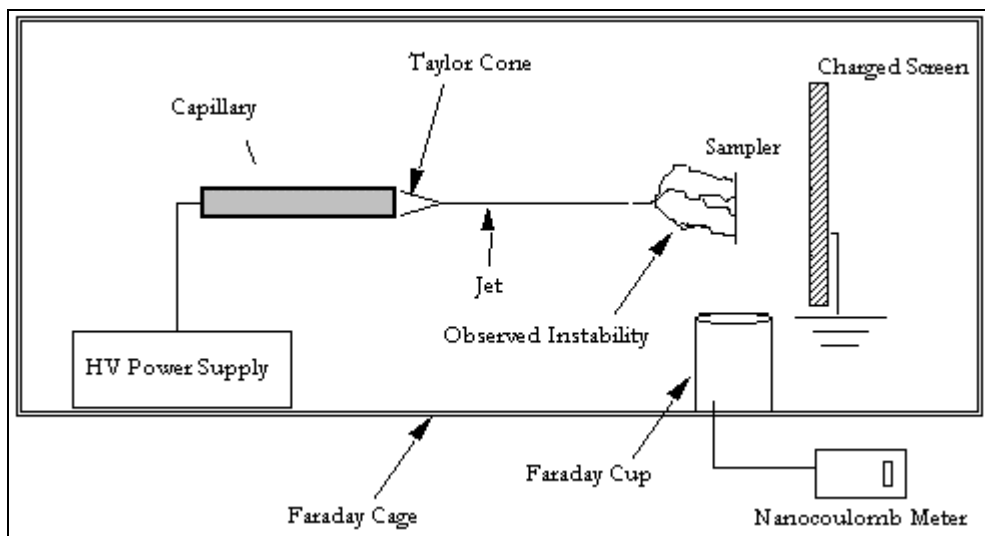


Figure 1: UMD electrospinning configuration.

2. Fluids

A wide range of fluids can be spun by the electrospinning technique. In the current project, the UMD/MIT team has focused most recently on solutions of polycaprolactone (PCL) and polyacrylonitrile (PAN). At MIT, solutions of PCL in 3:1 chloroform:methanol, 3:1 toluene:methanol, and 3:1 dichloromethane:methanol mixed solvents are also used. Tetrabutylammonium perchlorate (TBAP) is used to vary the conductivity of these solutions. At UMD, PCL in acetone and PAN in dimethylformamide are used as spin solutions.

3. Experimental characterization methods

Quantitative analysis of the electrospinning process falls into three categories. These are described in detail in a previous report [12] and consist of the following:

(1) *Solution properties*. The relevant fluid properties are density, viscosity, surface tension, permittivity, conductivity and viscoelasticity. Of these, viscosity and conductivity appear to play the greatest role in the electrospinning of dilute solutions. For all the electrohydrodynamic

modeling studies, the solutions used were confirmed to be non-shear-thinning for the range of wall shear rates expected to occur in the spinnerette.

(2) *Operating parameters.* The relevant operating parameters are flow rate, electric field strength, and electric current flow between the spinnerette and collector. The volumetric flow rate is closely controlled through the use of the syringe pump. Field strength may be varied by changing either the applied voltage or the distance over which the voltage drop to ground occurs. Both variables have been studied. Thinning of the jet depends principally on the field strength; however, the development of instabilities in the jet requires sufficient distance of travel for the instabilities to grow in amplitude. The total electric current contains contributions from both convection and conduction currents, and provides an indirect measure of the total surface charge density on the jet. Surface charge density, in turn, is believed to play a major role in determining jet stability. At MIT, jet current is measured by monitoring the voltage drop across a resistor between the collector and ground, and correcting for any ionization current which occurs at zero flow. At UMD, charge per unit mass is measured as described above.

(3) *Fiber characterization.* Fiber diameter distributions are measured using scanning electron microscopy. For example, at MIT samples of nonwoven webs were coated with gold-palladium using a Denton Vacuum Desk II sputtering machine and observed using an AMRAY 1200B scanning electron microscope (SEM). Fiber diameters were sampled by measuring the width of those fibers intersected by a straight line drawn at random across the image. Fibers were also observed using a Leica DMRX polarized optical microscope with Sernamount compensator, green filter (546 nm) and Zeiss Microfilair Microcode eyepiece. Fibers were observed in a mounting liquid with refractive index 1.546. Porosity (the ratio of void volume to bulk volume) is calculated from the sample weight and bulk volume. Pore size distribution was measured at Porous Materials, Inc. (PMI) using their capillary flow porometer. At UMD, crystallinity has been monitored by differential scanning calorimetry (DSC).

Mathematical modeling

In our continuing collaboration with M.P. Brenner (School of Applied Sciences, Harvard University) we have focused on modeling the jet profile in the stable region and clarifying the role of the jet shape near the nozzle on the subsequent evolution of the jet. This serves to extend our previously reported model of the electrospinning process, wherein results for jet profile some distance from the nozzle, and the onset of the whipping instability were adequately described [14-16]. Both numerical solution for the jet profile and some analytical scaling models are being developed. To date, electric current I has been considered as an independent process parameter in the modeling. In reality I is set by the electric resistivity of the jet. The resistivity of the jet is due to the conventional electric resistivity and the effective "advection" resistivity. The former is dominant in the nozzle domain, where most of the charges are distributed through the jet's volume. Far from the nozzle, charge resides predominantly on the jet surface and is convected together with the fluid mass, and the resistivity is controlled by surface charge density and flow rate. The cross-over from the electric resistivity regime to advection resistivity regime occurs at a distance L from the nozzle, whose scaling relationship can be expressed as follows:

$$L^5 = \frac{Q^6 \rho^2 K^4 \beta (\ln \chi)^2 h_0^3}{I^5 E_\infty}$$

where Q is the flow rate, ρ is the fluid density, K is the fluid conductivity, β is a measure of the dielectric discontinuity across the jet surface [15], χ is the ratio of jet length to nozzle diameter h_0 . I is the electric current and E_∞ is the applied electric field

Significantly, we find that the jet behavior near the nozzle is sensitive to operating conditions, jet geometry and fluid properties. However, far from the nozzle, the scaling for the radius of the jet h is determined mainly by operating conditions:

$$h = \left[\frac{\rho Q^3}{2\pi^2 I E_\infty} \right]^{1/4} z^{-1/4}$$

where z is the distance from the nozzle.

Experimental results

Jet current: Jet currents have been measured as functions of flow rate under different conditions. Fig 2 shows the current dependence on flow rate for stable whipping of 15% PCL in 3:1 toluene:methanol. Two regimes are suggested in the figure. At lower flow rate, the current increases non-linearly with the flow rate, while at high flow rate, the current is linearly dependent on flow rate as observed previously for glycerol and PEO/water [13], indicative of a constant induced charge density above a certain flow rate for a given field strength. The corresponding charge densities, I/Q , are on the order of $10 \mu\text{C}/\text{cm}^3$, intermediate between those reported previously for glycerol and PEO/water solutions [13]. The induced charge density increases at a rate of $6 \mu\text{C}/\text{cm}^3$ at high flow rates for $E=1.67 \text{ kV}/\text{cm}$. Charge densities measured at UMD using the Faraday cup method for PAN in DMF are shown in Fig 3; the values are comparable to those deduced from Fig. 2 for PCL in 3:1 toluene:methanol. Linear dependence was also observed for current as a function of applied field [13]. Spinnerettes of different length were used to test the dependence on contact time of the transfer of charge from the spinnerette to fluid. For spinnerettes of length 5 and 10 cm, no difference was observed in the current–flow rate relationship, indicating that the time needed for charge transfer from the spinnerette is small compared to the contact time.

Fiber diameter and morphology: Figure 4 shows a SEM micrograph for PCL fibers spun from a 13 wt% solution in acetone. This case appears to be intermediate between a bead-forming jet and a strongly thinning, fiber forming jet. DSC applied to these fibers indicates that they are semicrystalline. Figure 5 shows the dependence of the final fiber diameter on flow rate for three different PCL solutions. While the average fiber diameter increases with the flow rate, it appears to saturate at high flow rate. The reasons for this behavior are being investigated.

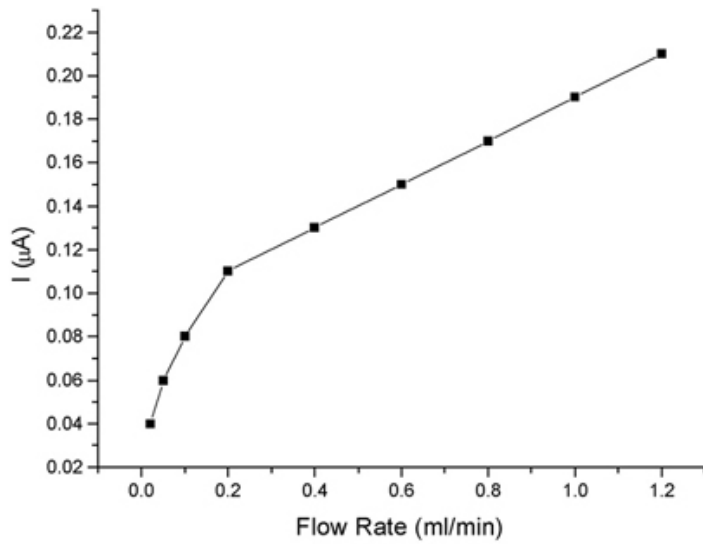


Figure 2. Electric current versus flow rate for stable whipping of 15% PCL in 3:1 toluene:methanol. $E=1.67$ kV/cm.

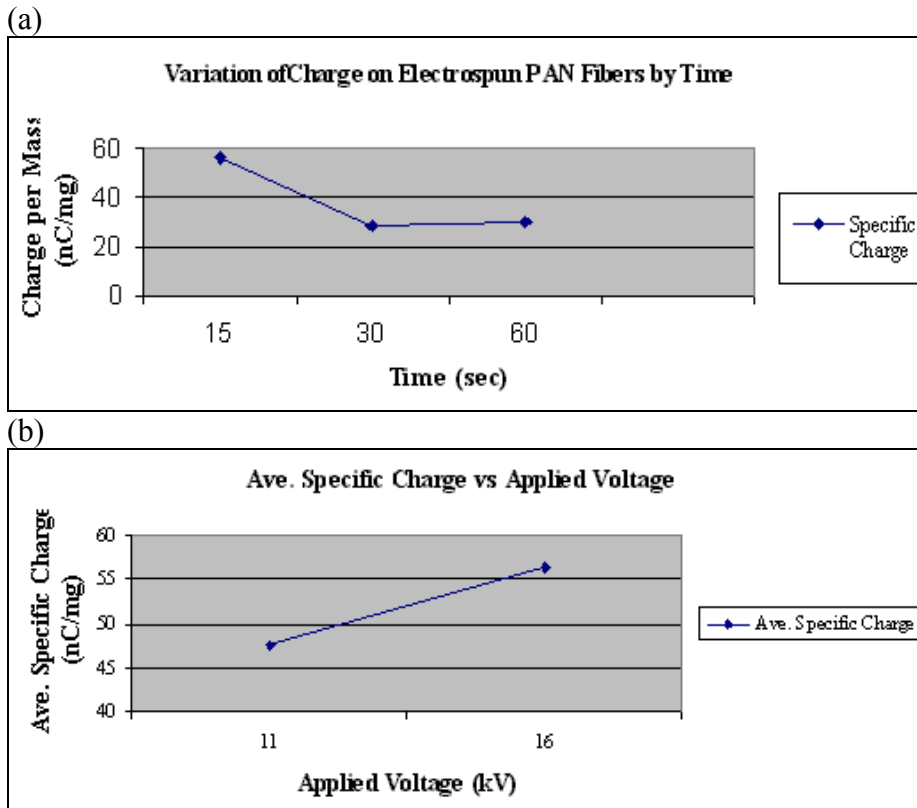


Figure 3. Charge per unit mass for electrospinning an 8 wt % solution of PAN in DMF: (a) as a function of collection time; (b) as a function of applied voltage for 15 s collection time. $Q=0.005$ ml/min, $d=15.5$ cm, $T=23$ °C, relative humidity=82%. (Faraday cup method).

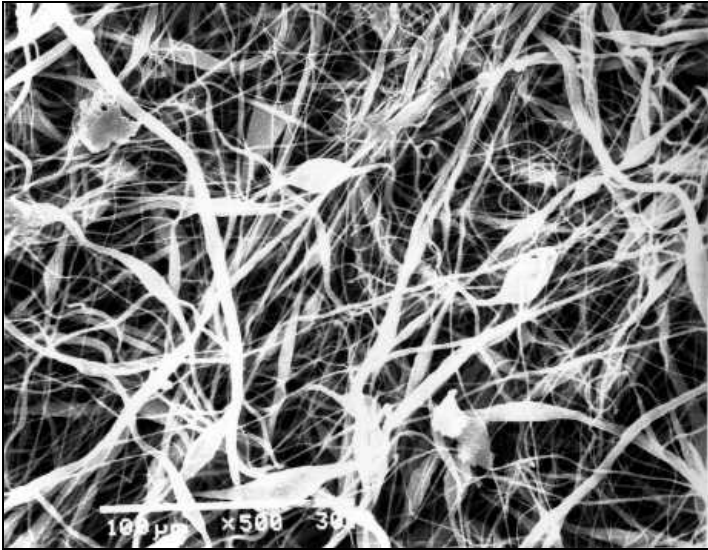


Figure 4: SEM of PCL fibers electrospun from 13 wt % PCL/acetone solution.

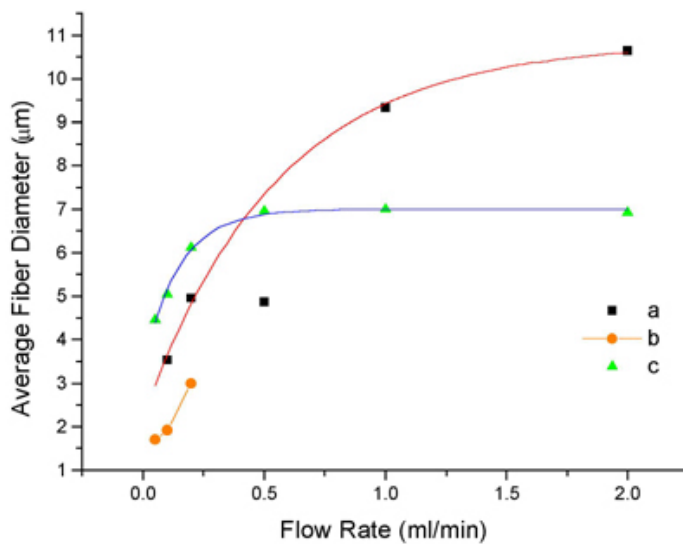


Figure 5. Average fiber diameter versus flow rate for different fluids, (a) 15% PCL in 3:1 dichloromethane:methanol (b) 12% PCL in 3:1 dichloromethane:methanol (c) 20% PCL in 3:1 chloroform:methanol

Models of the electrospinning process indicate that the final fiber diameter should be strongly dependent on the amount of charge present in on the jet. Coulombic repulsion between charges and torques arising from the interaction of charge with the electric field are among the mechanisms proposed to be responsible for diameter reduction. On the premise that charge induction is primarily a function of solution conductivity, we have performed studies of PCL solutions in which conductivity is varied through addition of TBAP. Fig. 6 shows how conductivity varies with TBAP addition in PCL/chloroform solutions. The resulting changes in

fiber diameter for fibers electrospun from solutions of varying conductivity are then shown in Fig 7. From this data, it appears that the relation between conductivity and fiber diameter is not a simple one. One possible explanation hinges on the different roles of conductivity and charge relaxation to the surface in the "nozzle regime", $L < 1$.

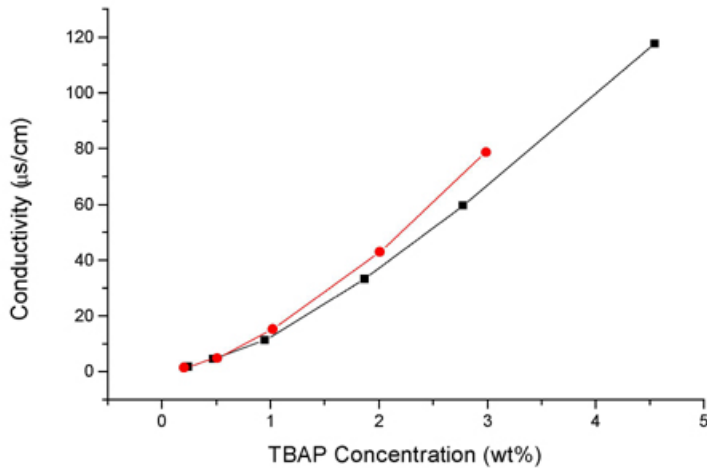


Figure 6. Conductivity versus TBAP concentration (a) in black, 10% PCL in 3:1 toluene:methanol; (b) in red, 15% PCL in 3:1 toluene:methanol

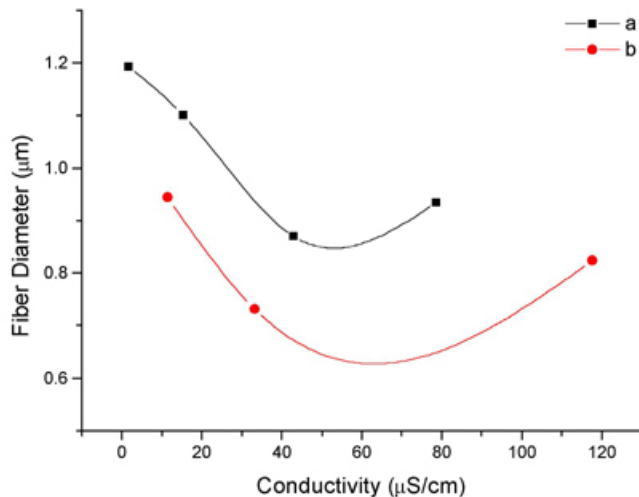


Figure 7. Average fiber diameter versus conductivity. (a) in black, 10% PCL in 3:1 toluene:methanol (b) in red, 15% PCL in 3:1 toluene:methanol. The curves are drawn as guides to the eye.

Porosity: High porosity and small pore size are potential advantages of electrospun fabrics compared to other materials. Fig. 8 shows the pore size distribution of a PCL nonwoven fabric measured using a capillary flow porometer. The predominant pore size is confirmed to be on the order of magnitude of the fiber diameter. The porosity of this sample was found to be 88%. Such samples are readily produced by electrospinning technology.

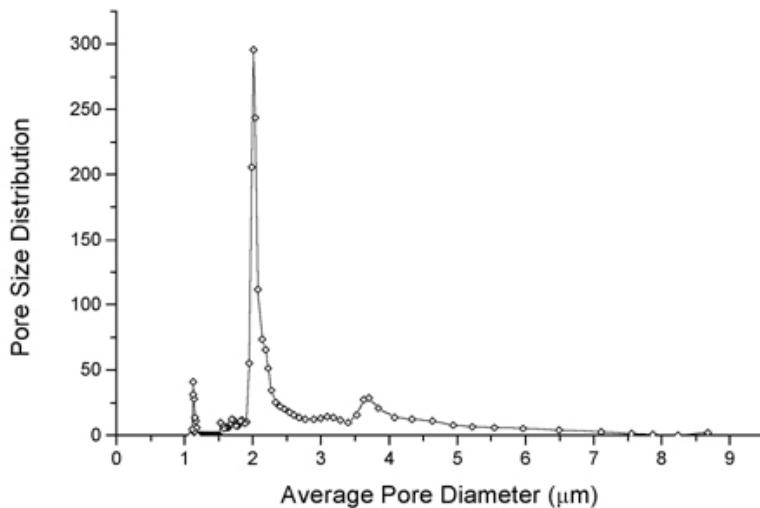


Figure 8. Pore size distribution of PCL electrospun fibers. The sample was made from 15wt% PCL in 3:1 Dichloromethane:Methanol solution.

Conclusion and Outlook

In this study, experiments are being performed to study the correlation between fiber properties and control parameters. While the physics of the instabilities in electrically driven jets is rather well understood, the issue of what sets the electric current and how the electric current and the surface charge density are linked with the fiber diameter remains a puzzle. Our experimental data shows that electric current vs flow rate and electric current vs fiber diameter dependences are correlated. Investigations are on-going to further elucidate the connection between the current and the fiber diameter via experimental and theoretical approaches.

Acknowledgements

The authors are grateful to the National Textile Center for financial support of this project, under US. Department of Commerce Grant 99-27-7400.

Web site: <http://heavenly.mit.edu/~rutledge/electrospin.html>

References

- [1] A. Formhals, US Patent 1,975,504 (1934)
- [2] G. Srinivasan, D.H. Reneker, *Polym. Int.*, 36, 195 (1996).
- [3] D.H. Reneker, I. Chun, *Nanotechnology*, 7, 216 (1996).
- [4] J. Doshi, D.H. Reneker, *J. Electrostatics*, 35, 151 (1995).
- [5] H. Fong, I. Chun, D.H. Reneker, *Polymer*, 40, 4585 (1999).
- [6] H. Fong, D.H. Reneker, *J. Polym. Sci.-Phys.*, 37, 3488 (1999).
- [7] R. Jaeger, M.M. Bergshoef, C. Martin-I-Batlle, D. Schoenherr, G.J. Vancso, *Macromol. Symp.*, 127, 141 (1998).
- [8] L. Larrondo, R. St. John Manley, *J. Polym. Sci. – Phys.*, 19, 909, (1981).
- [9] L. Larrondo, R. St. John Manley, *J. Polym. Sci. – Phys.*, 19, 921, (1981).
- [10] P.W. Gibson, H.L. Schreuder-Gibson, D. Rivin, *AIChE J.*, 45, 190 (1999).
- [11] J.-S. Kim, D.H. Reneker, *Polymer Comp.*, 20, 124 (1999).
- [12] S.B. Warner, A. Buer, M. Grimler, S.C. Ugbohue, G.C. Rutledge, M.Y. Shin, *NTC Annual Report*, Project M98-D01 (1999).
- [13] Y.M. Shin, M.M. Hohman, M.P. Brenner and G.C. Rutledge, *Polymer*, 42, 9955 (2001).
- [14] M.Y. Shin, M.M. Hohman, M. Brenner and G.C. Rutledge, *Appl. Phys. Lett.* 78, 1149 (2001).
- [15] M.M. Hohman, Y.M. Shin, G. Rutledge and M.P. Brenner, *Phys. Fluids* 13, 2201 (2001).
- [16] M.M. Hohman, Y.M. Shin, G. Rutledge and M.P. Brenner, *Phys. Fluids* 13, 2221 (2001).